Journal Of Harmonized Research (JOHR)

Journal Of Harmonized Research in Applied Sciences
3(1), 2015, 66-73

ISSN 2321 – 7456

Original Research Article

STRUCTURAL PROPERTIES COMPARISON OF BORON AND ALUMINUM CO-DOPED ZINC OXIDE FILMS DEPOSITED ON POROUS SILICON AND SILICON SUBSTRATE

Rashid Hashim Jabbar[1] and Anwar Hussein Ali [2]

[1] Center of Applied Physics, Ministry of Science and Technology, Baghdad, Iraq.
[2]Dept. of Physics, College of Science, Al-Mustansiriyah University, Baghdad, Iraq.

Abstract: This paper presents the comparison of structural properties between silicon and porous silicon(PS) structural substrates used in the same conditions to deposition of aluminum boron co-doped ZnO (AZB) thin films of nanostructures with doping (2,4,6,8 at %.)Deposited at 450 ^{o}C on silicon and porous silicon substrates by chemical spray pyrolysis in (150±5 nm) thickness. The structure of AZB nanostructure films has been found to exhibit the hexagonal wurtzite structure. The surface topography of the films and the porous silicon was studied by using the Scanning Electron Microscopy (SEM), Transmission electron microscopy (TEM) and the Atomic Force Microscopy (AFM), the surface concentration shows that the roughness of the thin films increase with the increase of doping concentrations. The structural details and microstructure were obtained from X-ray diffraction, the results shows the grain size decreased with the increase of doping concentration.

Keywords: porous silicon, PS, ZnO nanostructures, boron and aluminum co-doped, structural properties.

Introduction:

Porous silicon has attracted great deal of interest due to efficient room-temperature visible photolumiencence, which for the first time was observed by Canham in 1990 [1]. Holes pile up at the Si-HF interface and electro polishing occurs. For all the three conditions mentioned above the holes play an important role: in fact, PS formation is a self-regulated mechanism, with hole depletion as the limiting agent. The dissolution reaction begins at defects on the Si wafer surface; the pores are formed and their walls are eroded until they are emptied of the holes. (PS) is macroscopically and empirically characterized by its porosity [2].

Porosity is defined as the fraction of void within the porous silicon layer. As a general rule, the samples in the low porosity range from 0 to 30 %, the medium porosity range from 30 to 70 %, and the high porosity range is from 70 to 100%. However, when the porous silicon layer is thin (200 nm), the mass difference is the same order of magnitude as the error in measurements, and the porosity value obtained is unreliable. Porosity is greatly affected by the anodization

For Correspondence:
rasheed2045@googlemail.com
Received on: February 2015
Accepted after revision: March 2015
Downloaded from: www.johronline.com

current density, etching time and hydrofluoric acid concentration. Measure the film thickness is by direct determination using the scanning electron microscopy (SEM) or atomic force microscopy (AFM) [3].

Experimental*:*

N-type and p-type Si with resistivity (ρ= 0.05 – 0.1 Ω.cm) and (111) crystalline orientation is employed as substrates with dimensions of (2 x 2cm^2) to prepare PS using photochemical etching process. The thickness is about 500 μm. A 0.075M concentration precursor solution of zinc nitrate (Zn $(NO_3)_2.6H_2O$ is a solid material which has a white color and its molecular weight (297.4 g/mole)) dissolved in distilled water. A magnetic stirrer is incorporated for this purpose for about (10-15) minutes to facilitate the complete dissolution of the solute in the solvent. The weight is measured via an electrical balance sensitive four digits (10^{-4}gm). The used precursor for the *Boron* is the Acidic Boron (H_3BO_3 – 99.8% purity).

The spray pyrolysis substrate temperature is maintained within (450 ±10 ^oC) during the deposition. Film thickness is controlled by both the concentration of molarities and the number of sprays. (3) Seconds spray time is maintained during the experiment then waiting for (42) seconds where this time was enough to return the substrate temperature to (450 ±10 ^oC). The normalized distance between the spray nozzle and substrate was fixed at 28cm, AZB nanostructure films of AZB (0.0, 2, 4, 6, 8 at %) i.e.[ZnO pure, ZnO:(B 1%+Al 1%),ZnO:(B 2%+ Al 2%),ZnO:(B 3%,Al 3%), ZnO:(B 4%,Al 4%)].

The photochemical etching process is electrodeless since there is no applied bias voltage during the etching process. This process is carried out using ordinary light source. A simple setup in our experimental has been used for the photochemical etching process. The setup consists of a Quartz Tungsten Halogen lamps (100W) integrated with diluted etching acid in Teflon container as shown in figure (1). Thin homogenous PS layer of various thickness were formed on the frontal surface of the material using two methods electrochemical (EC) and photoelectron chemical (PEC). PS layers of different structures and properties were synthesized using halogen lamp for PEC process of silicon. The porous silicon prepared by electrochemical and Photo electrochemical etching with 30 mA for 30 minutes.

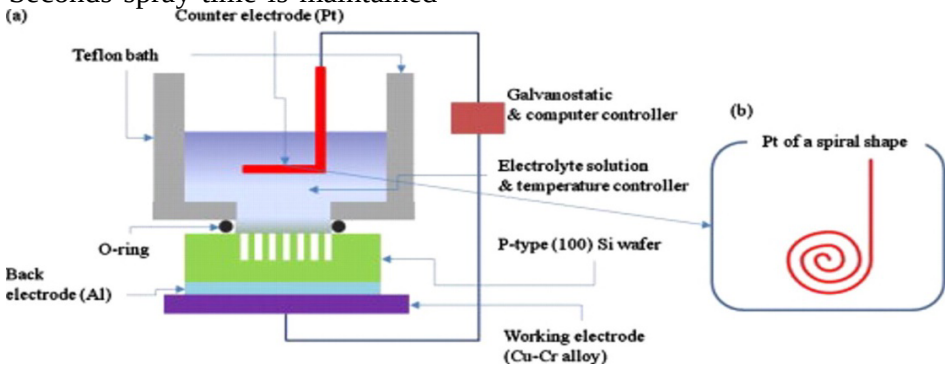

Fig. (1): Electrochemical etching cell set-up

3. Result and discussion:

Figure(2, a ,b)) revealed X-ray diffraction analysis of ZnO and AZB thin films as a function of aluminum and boron co-doped concentration firstly, and type of the substrate secondary, the figure shows the existence of the (002) orientation plane for silicon substrate at undoped ZnO and AZB(2 and 4 at %.), wihle only in undoped ZnO (002) and (101) orientation planes appear, according to the XRD data in table(1) are (100), and (101) respectively, this means the thin films are

polycrystalline with a hexagonal wurzite structure compared with standard (ASTM) of ZnO card, the (002) plane is the preferred orientation observed for all the thin films prepared.

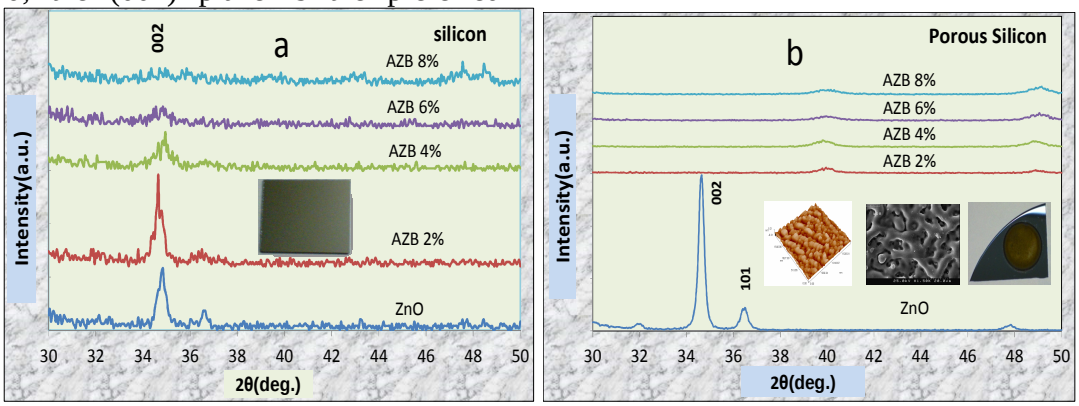

Fig. (1): XRD patterns of ZnO and AZB thin films deposited on: (a) silicon, (b) porous silicon substrate with doping concentration: 0.0 to 8 at. %.

Table (4-1): Structural parameters of ZnO and AZB thin films deposited on siliconand porous silicon substrates at 450 ^{o}C.

hkl	*Sample*	*2θ (deg.)*	*d(nm)*	*β(FWHM) (deg.)*	*a(nm)*	*c(nm)*
	Silicon substrate					
002	ZnO	34.8139	0.25948	0.43	0.32181	0.51558
	AZB: 2%	34.6667	0.26004	0.20	0.32357	0.51840
	AZB: 4%	34.9380	0.25980	0.25	0.32287	0.51728
	Porous silicon substrate					
002	ZnO	34.6459	0.258701	0.2744	0.33957	0.54404
101	ZnO	36.4679	0.246183	0.3481	0.32314	0.51771

The average grain size D_g was calculated by Scherer equation [4]:

$$D_g = \frac{k\lambda}{\beta cos(\theta)} \quad \text{…….. (1)}$$

Where $k = 2\sqrt{\frac{\ln(2)}{\pi}} = 0.94$ called(Scherer's constant), λ is the wave length of incident X-ray radiation , β is the intrinsic full width at Half Maximum of the peak , and θ is the Bragg's diffraction angle of the respective XRD peak .Assumes the world Warren that the mathematical representation of curves resulting from the X-ray diffraction (XRD) depends primarily on the amount of similarity between these curves and functions of each of the Cauchy and Gauss, in the case considered curve X-ray diffraction is similar to function Cauchy and take the form of $\frac{1}{\sqrt{1+k^2x^2}}$, the correction is given by the following relationship, which was called (Scherer's correction):

$$\beta_{cs} = \beta_m - \beta_i \quad \text{…… (2)}$$

Where: β_m is the measured full width at Half Maximum of the peak is, β_i is the instrumental broadening [5], where (β_i) = 0.11 deg.) for the used instrument. Compensation equation (2) in the relationship (1) we get:

$$D_g = \frac{k\lambda}{(\beta_m - \beta_i)\cos(\theta)} \quad \ldots\ldots\ldots (3)$$

In the case considered X-ray diffraction curve similar to the function Gauss which takes the form ($e^{-k^2x^2}$) the accuracy to be higher because of the great similarity between this function and the diffraction curves; it was suggested (Warren correction) form:

$$\beta_{cs}^{\ 2} = \beta_m^{\ 2} - \beta_i^{\ 2} \quad \ldots\ldots\ldots (4)$$

This correction called (Warren's Correction). Compensation equation (4) in the relationship (1) we get:

$$D_g = \frac{k\lambda}{\sqrt{\beta_m^{\ 2} - \beta_i^{\ 2}}\cos(\theta)} \quad \ldots\ldots (5)$$

Since the output line shape does not resemble the Gauss curve and Cauchy curve completely, so these relations have limited operation values. If the intensity curve does not sharp may be used (Scherer's correction) or (Warren's Correction) former because the difference between the values given by relations (3) and (5) is not large, which means that the decrease of the curve breadth (an increase of sharpness) means that the effect of the amount (β_i) is significant, since the width of the curve in the half intensity (FWHM) is inversely proportional with grain size according to equation (1), the decrease in (FWHM) leads to increase in the grain size, which means that few crystal defects are present in the sample. Moreover, Warren was suggested a relationship takes into account the geometric meaning which is [6, 7]:

$$\beta_{cs} = \sqrt{(\beta_m - \beta_i)\sqrt{(\beta_m^{\ 2} - \beta_i^{\ 2})}} \quad \ldots\ldots (6)$$

Compensation equation (6) in the relationship (1) we get:

$$D_g = \frac{k\lambda}{\sqrt{(\beta_m - \beta_i)\sqrt{(\beta_m^{\ 2} - \beta_i^{\ 2})}\cos(\theta)}} \quad \ldots\ldots (7)$$

The average grain size and micro strain of (100), (002) and (101) planes using equations (1, 3, 5 and 7) is in the table (2).

Table (2): Average Crystallite size and micro strain of (002 and 101) planes of ZnO and AZB thin films deposited on silicon and porous silicon substrate.

hkℓ	***Sample***	***average crystallite size(nm)***			
		eq.(1)	***eq.(3)***	***eq.(5)***	***eq.(7)***
		silicon substrate			
002	ZnO	20.2	27.0	20.8	23.7
	AZB 2%	43.8	98.2	52.6	71.8
	AZB 4%	34.8	62.2	38.8	49.1
	AZB 6%	7.76	8.61	7.80	8.20
		Porous Silicon substrate			
002	ZnO	31.7	52.9	34.6	42.8
101	ZnO	25.1	36.7	26.5	31.2

Figures (2) shows the Images of p-type and n-type of porous silicon (PS) prepared for 30 minutes at 30m A/cm^2 etching current densities before and after deposit ZnO at 450 ºC.

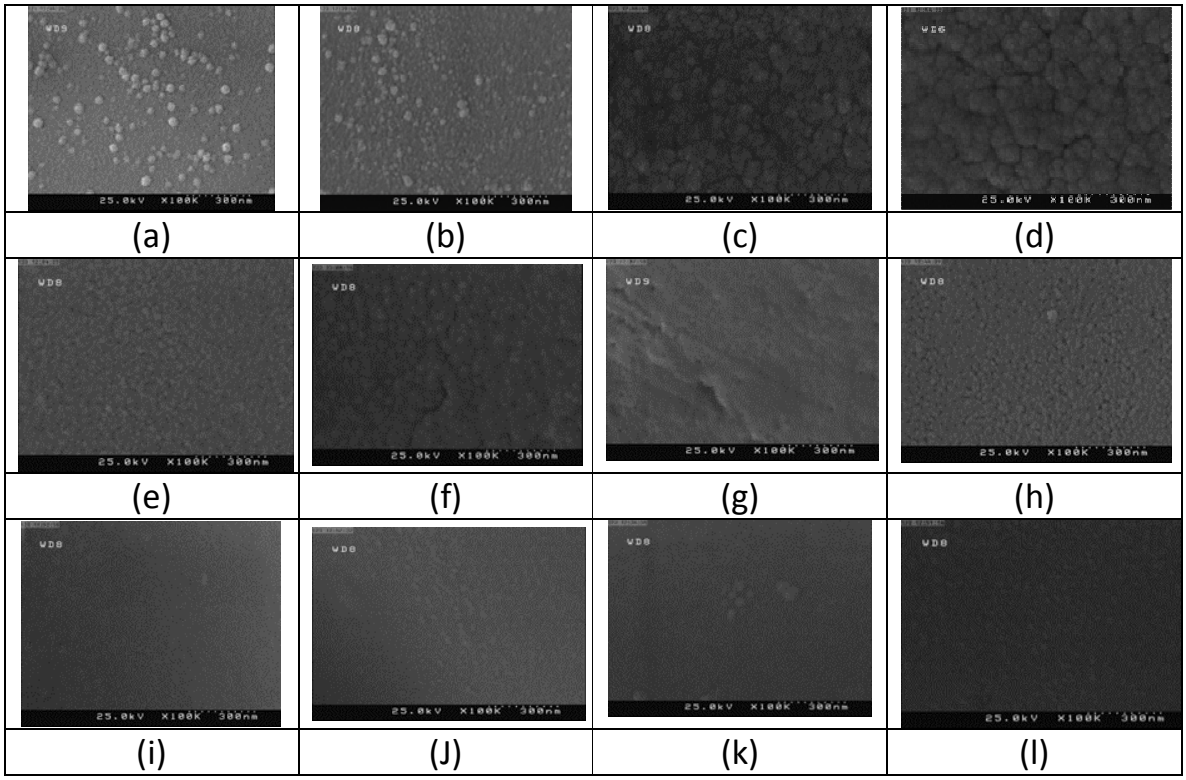

Fig.(2) SEM of: a) n- PS, b)p- PS, c) ZnO/n-PS, d)ZnO/p-PS, e) AZB 2%/n-PS, f) AZB 2%/p-PS, g) AZB 4%/n-PS, h) AZB 4%/p-PS, i) AZB 2%/ n -PS, j) AZB 8%/p-PS, k) AZB 8%/ n -PS, l) AZB 8%/p-PS deposited at 450°C.

The porosity of the porous silicon calculated by the equation: $Porosity\% = \frac{m_1 - m_2}{m_1 - m_3}$, the weight of the virgin wafer is measured before anodization (m_1), then after anodization (m_2), and finally after dissolution of the porous silicon layer (m_3) in a 1m solution of sodium hydroxide (NaOH)[8]. the thickness of the porous silicon layer is calculated by the empirical equation $T_{Psi} = K * {J_{PSi}}^{m} * t$, Where: T_{Psi} is thickness of the PS layers in (cm), J_{PSi} is etching current density in (mA/cm^2) and t is etching time (sec.)[9]. Constants K and m are tabulated in table (2) and depend on HF concentration, and etching rate is calculated by the equation ($v_{PSi} = \frac{T_{PSi}}{t}$), where: v is etching rate (µm/min). Porosity, etching rate and thickness of the porous silicon layer are shown in table (3) [10-14].

Table (2): Coefficient determined for the empirical Eq. [15, 16].

HF concentration (%)	K (cm^3/mA.s)	m
30	1.01 x 10^{-7}	0.98
40	1.05 x 10^{-7}	0.96
50	1.13 x 10^{-7}	0.92

Table (3): Porosity, etching rate and thickness of the porous silicon layer.

Sample	T_{PS} (µm)	Porosity (%)	ν(µm/min)
PS	46.48	61-66	1.55

Transmission electron microscope (TEM) of ZnO morphologies were revealed to be spherical, hexagonal and rod-like. The presence of ZnO spherical nanoparticles along with a few nanorods was observed as shown in figure (3). The crystallite sizes of spherical particles were found to be in the range of 6.5–23 nm.

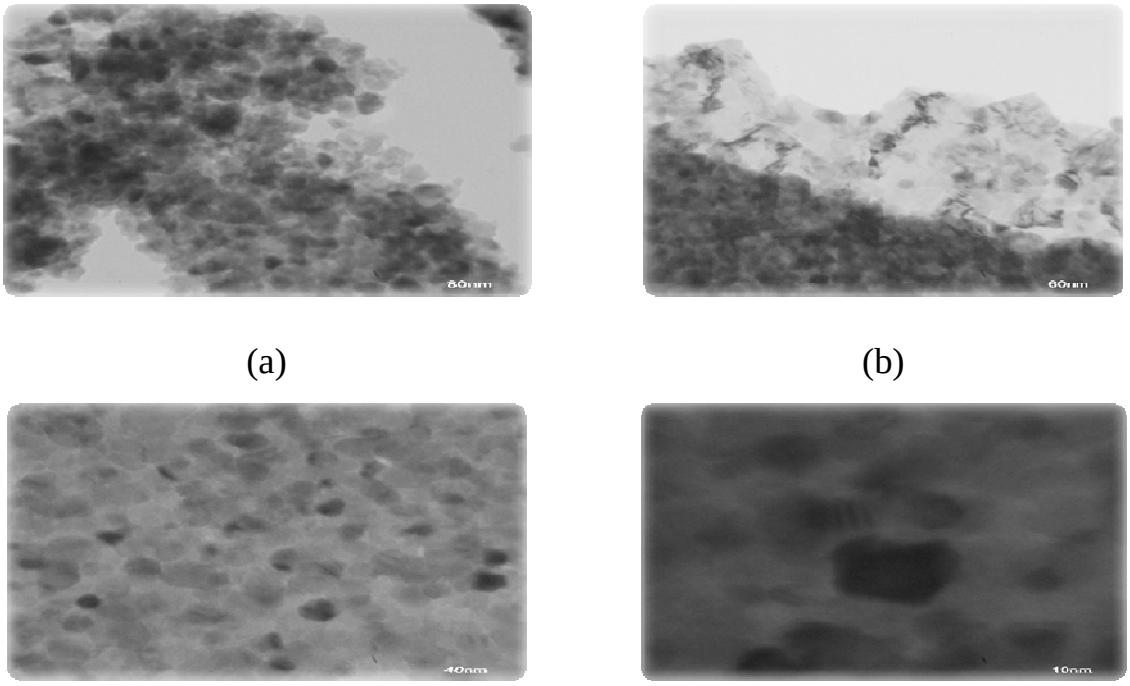

(a) (b)

(c) (d)

Fig. (3)TEM image of undoped ZnO for a different scales: (a) 80 nm, (b) 60 nm, (c) 40 nm, (d) 10 nm.

Figure (4) shows (AFM) for the thin films deposited on the porous silicon, the granularity distribution, (2-D) and (3-D) AFM images of ZnO and AZB thin films with the co-doped (2, 4, 6 and 8) %, deposited on PS prepared at 450 ºC.

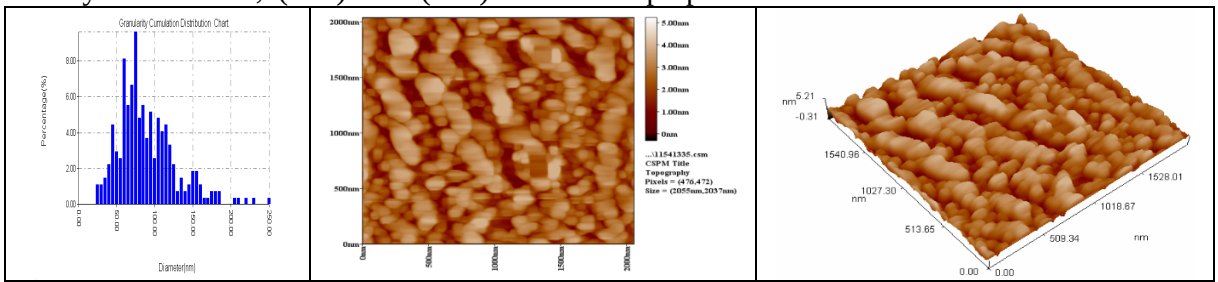

PS

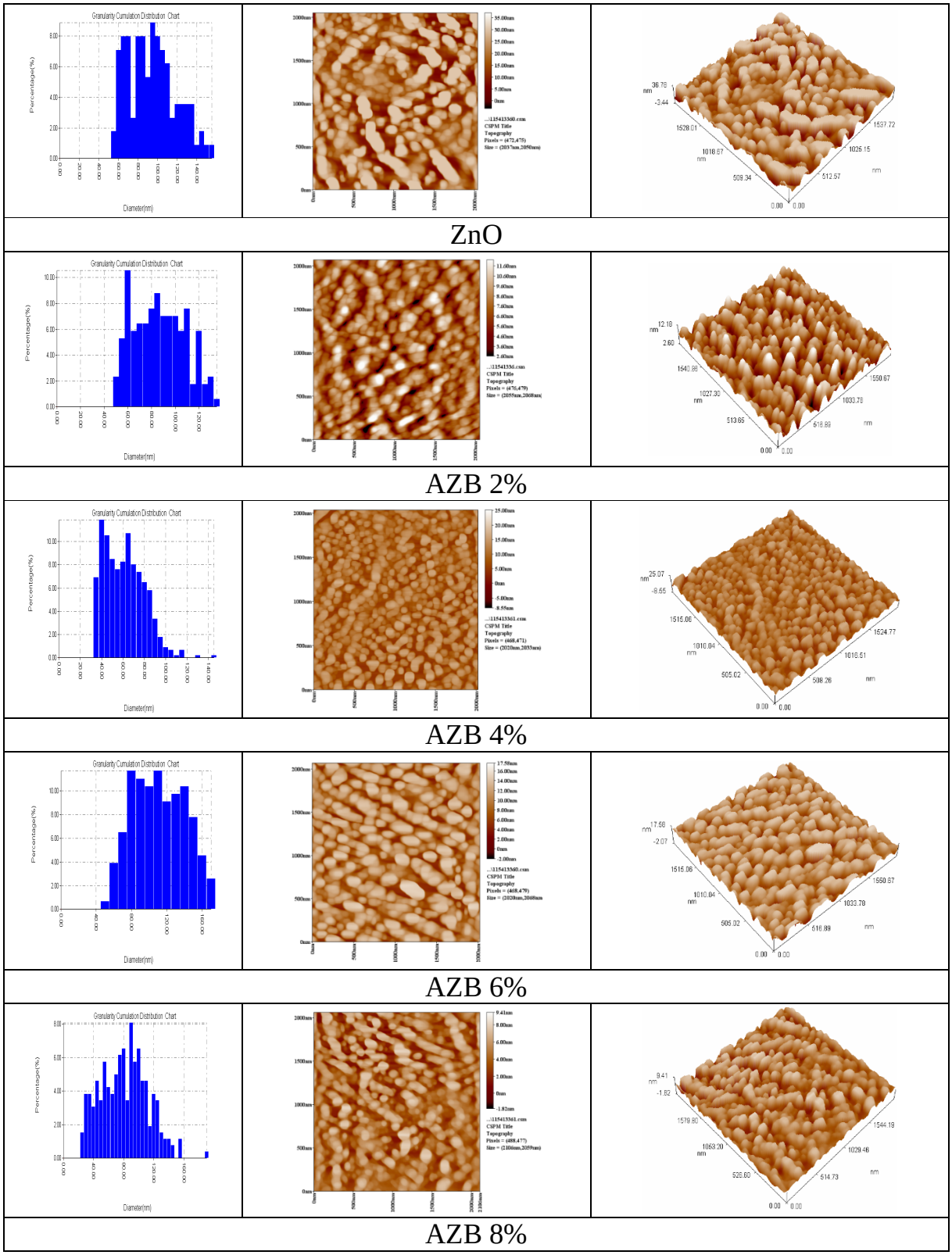

Fig. (4): Granularity distribution, 2-D and 3-D AFM image of the ZnO and AZB thin films with doping concentration (2, 4, 6, and 8) % deposited on N-PS at 450 °C.

The AFM measurement show the average grain size decrease with increase of aluminum and boron doping concentration within the range (*90.7-26.31 nm)* and the roughness is increased with increase of doping concentrations within the range (1.34-6.15 *nm).*

4. Conclusions:

The surface topography of the thin measured by (SEM), (TEM), (AFM) and (XRD) shows the thin films are nanostructure for undoped ZnO and aluminum-boron codoped ZnO, and the grain size is decrease with the increase of co-doping concentrations. Only (002) orientation plane is growth on silicon substrate for undoped ZnO and AZB (2 and 4 at %.) and (002) awhere the grain size of ZnO pure is less than AZB (2 and 4 at %). It was found that the increase of concentration of Al and B due to decrease of microstrain on glass substrate and increase on silicon substrate for (002). the interplaner spacing of (002) plane for AZB(2 and 4 at%) on glass substrate be greater than the interplaner spacing on silicon substrate.

References

[1] V Lehmann and U Gösele, "Porous silicon formation: a quantum wire effect", App Phys Lett, Vol 58, No 8, pp. 856-858, 1991.

[2] C. Vinegoni, M. Cazzanelli and L .Pavesi"Porous silicon microcavities", Universit`a di Trento, Trento, Italy, 2000.

[3] S. E. Foss, "Graded Optical Filters in Porous Silicon for use in MOEMS Applications", PhD Thesis, University of Oslo, Oslo, Norway September, 2005.

[4] H. J. von Bardeleben and M. Schoisswohl, "Porous Silicon Science and Technology", edited by J. C. Vial and J. Derrien, Springer-Verlag, Berlin, pp. 225, 1995.

[5] James R. Connolly, "Elementary Crystallography for X-Ray Diffraction" EPS400-002, (2012)

[6] S MONDAL, S R BHATTACHARYYA and P MITRA, "Effect of Al doping on microstructure and optical band gap of ZnO thin film synthesized by successive ion layer adsorption and reaction", PRAMANA journal of physics, Indian Academy of Sciences Vol. 80, No. 2,—February (2013) pp. 315–326

[7] L.V. Azarooff. (1968). Mc Graw-Hill Book Company. 552-556.

[8] Th.H.DE.Keijser. (1982). J. Appl. Cryst., 15, 308-314.

[9] Petra Granitzer and Klemens Rumpf," Porous Silicon—A Versatile Host Material", Materials, Vol. 3, pp. 943-998, 2010.

[10] C. Suryanarayana and M.G. Norton, "X-ray Diffraction A Practical Approach", Plenum Press, New York, pages 207-221, 1998.

[11] B.D. Cullity and S.R. Stock, "Elements of X-ray Diffraction, 3rd Edition", Prentice-Hall, Upper Saddle River, NJ, Ch. 5, pages 167 and Ch. 14, pp. 385 402, 2001.

[12] Mittemeijer, E.J. and P.Scardi,"Diffraction Analysis of the Microstructure of Materials", Springer Seriesin Materials ScienceVol. 68, Springer-Verlag, Berlin Heidelberg New York, 2004.

[13] Lucks, I., P. Lamparter, J. Xu and E.J. Mittemeijer," XRD Line Broadening Analysis with Ball Milled Palladium", Materials Science Forum 443-444, pp.119-122, 2004.

[14] Jasmeet Kaur, Praveen Kumar, Thangaiah Stephen Sathiaraj and Rengasamy Thangaraj," Structural, optical and fluorescence properties of wet chemically synthesized ZnO: Pd2+nanocrystals",Kaur et al. International Nano Letters, 3:4, 2013.

[15] M. J. Sailor," Porous Silicon in Practice: Preparation, Characterization and Applications",First Edition, 2012.

[16] O. Tobail,"Porous Silicon for Thin Solar Cell Fabrication", Institut für physikalische elektronik der universität stuttgart 2008.